SIMILARITIES AND DIFFERENCES OF EPOXY RESIN NANOCOMPOSITES WITH CNTS AND BNNTS

J. W. Guan[1*], B. Ashrafi[2], Y. Martinez-Rubi[1], M. B. Jakubinek[1], K. Laqua[2], D. Park[2], M. Rahmat[3], K.S. Kim[1], M. Daroszewska[1], S. Walker[1], D. Ruth[1], M. Plunkett[1], C. T. Kingston[1] and B. Simard[1]

[1] Security and Disruptive Technologies Portfolio, National Research Council Canada, 100 Sussex Dr., Ottawa, Canada
[2] Aerospace Portfolio, National Research Council Canada, 5145 Decelles Av., Montreal, Canada
[3] Aerospace Portfolio, National Research Council Canada, 1200 Montreal Road, Ottawa, Canada

Keywords: Multi-walled Carbon nanotubes (CNTs), Boron nitride nanotubes (BNNTs), Epoxy resin, Nanocomposites, Mechanical property

ABSTRACT

Boron nitride nanotubes (BNNTs) are excellent one-dimensional hollow-structured nanomaterial similar to their CNTs counterparts in many aspects of their mechanical properties, but have differences in other aspects such as high thermal stability, transparency in visible light region and great neutron absorption. Unlike CNTs, BNNT-nanocomposites have few literatures due to the limited availability of BNNT-materials. In this work, the comparative studies of BNNT- and CNT-Epon828 composites were conducted in a bulk composite format by dispersing nanotubes in Epon 828 resin using acetone as a solvent with ultrasonication. After removal of solvent, the BNNT-Epon828 formulation was then mixed with curing agent by a planetary centrifugal mixer. The nanocomposites were fabricated as ~200 μm thin films using a metal shim (200 μm in thickness) to control the film thickness between two pre-treated borosilicate glass plates. The effects of nanotube type, loading and surface modification on the mechanical performance of the nanocomposites were determined. BNNT-Epon828 composites showed a better wettability, dispersity and consistently better fracture toughness than CNT-epoxy composites. In both CNT and BNNT cases, surface chemical modifications were clearly sensitive to the mechanical properties. In the case of OH-functionalized BNNT-Epon828 composites, an optimum BNNT concentration about 2 wt% offered the best mechanical performance.

1 INTRODUCTION

Common industrial epoxy resins such as MY0510 and Epon 828 have been successfully utilized in a wide range of industrial applications over the past few decades and are fast reaching their optimal performance limits. In challenge of industrial demands for lightweight and stronger composite materials, a promising alteration is to further improve their mechanical performance, along with adding multifunctional features like electrical and/or thermal conductivity, and increased thermal stability by forming multifunctional and structural composites through reinforcement with nanofillers such as carbon nanotubes (CNTs) and boron nitride nanotubes (BNNTs). Both CNTs and BNNTs are about 100 times stronger than traditional steel but only $1/6^{th}$ by weight. CNTs have been intensively studied and shown to have superlative mechanical, thermal and electrical properties [1, 2]. Great effort to harness the properties of CNTs in composites has been made over the past two decades, showing interesting mechanical and conductivity improvements [3, 4]. Generally, the primary factors limiting the overall performance improvement is due to the strong van der Waals interactions between nanotubes, which promote bundling, and the lack of interfacial interactions limited load transfer between nanotubes and matrix. The issues can be mitigated through chemical surface modifications [5-8]. While BNNT nanocomposites present many of these same challenges, recent works have reported more favorable interaction between BNNTs and epoxides [9-12], including easier wetting [11] and stronger interfacial shear strength [12], suggesting that BNNTs may be advantageous for reinforcing epoxy.

In addition, CNTs are black in color and start to combust around 400 °C in air. BNNTs, however, offer contrasting multifunctional advantages to CNTs, such as considerably high thermal stability, wide band gap (~6 eV) being an electrical insulator, high neutron absorption capability and no absorption in the visible light region. In applications such as transparent armor composites, aircraft and vehicle windows, transparency and high thermal stability are critical and BNNTs are advantageous. Research on BNNTs and their composites is limited and has fallen far behind to CNT counterparts [13]. One of the major reasons is that methods for large-scale production of CNTs were discovered in the early history of CNT development, which enabled the availability of CNTs in quantity from grams to kilotons [14], while even research-quantities of BNNTs are limited. In 2012, a break-through development of a pilot-scale RF-plasma production process at the National Research Council Canada (NRC) with a demonstrated capacity of ~ 200 g of BNNT material per day dramatically increased BNNT production capacity [15]. This and other recent approaches [16, 17] enable the availability of large quantity BNNTs now, which offers a great opportunity to advance research on BNNT chemistry, BNNT polymer composites and BNNT applications across a broad spectrum [11, 18-20]. In this study, we focused on a comparison study of the interactions of CNT and BNNT with Epon828 epoxy resin in a bulk format and in their cured composites, which eventually provides an opportunity for large scale production in the future, once the performance of BNNT-composite is optimized.

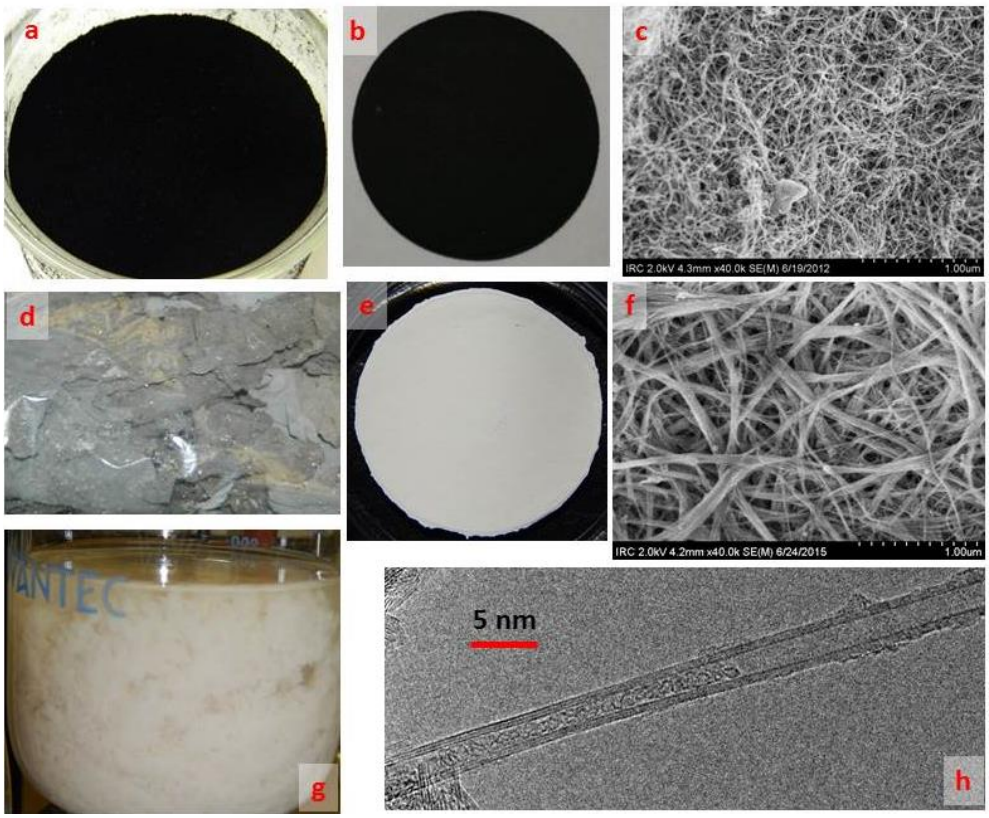

Fig. 1: a) loose, raw MWCNTs from Nanocyl (Belgium), b) CNT buckypaper made from a) by vacuum filtration in MeOH (~40 mm in diameter), c) SEM of CNTs as purchased, d) bulk BNNTs as produced at NRC, e) BNNT buckypaper made from the highly purified BNNT-suspension from g), f) SEM image of BNNTs from g), g) photo of highly purified BNNT-suspension in MeOH, and h) TEM image of an individual few-walled BNNT tube.

2 MATERIALS AND METHODS

Materials: a commercial epoxy resin (Epon828) and curing agent (Epikure 3223) were used in this study, and the portion of curing agent applied was 12 parts per hundred parts of resin (PPH) by

weight based on the optimized mixing ratio recommended by manufacturer. Fig. 1 shows photos and microscopy images of raw BNNTs, CNTs and their products. The raw BNNT material (Fig. 1d) was manufactured from an h-BN powder feedstock through an RF-plasma process as reported previously [8]. The raw BNNTs can be purified to high purity and estimated over 95% BNNT content by SEM analysis with snow-white color as shown in Fig. 1e, f and g by solvent extraction with ultrasonication. The BNNTs have high crystallinity, small diameters (~5 nm) and few walls (2-8 walls for the most population) (Fig. 1h). Highly purified BNNTs form a tougher BNNT-buckypaper that can be repeatedly bended and fully recover once the loading is removed as demonstrated in Fig. 2a, b and c. These BNNT buckypapers get wet much faster with epoxy resin than their CNT counterpart buckypapers as shown in Fig. 2d, e and f, where the epoxy resin visibly wicks through a horizontal BNNT buckypaper strip [21]. Purified BNNTs were also functionalized with OH/NH_2 groups by breaking their outer layer B-N network with a halogen treatment [22]. CNTs (NC7000™, MWCNTs) were purchased from Nanocyl (Belgium) and used as purchased without further treatment. As shown in Fig. 1a, b &c, the loose dry powder of CNTs material Fig.1a can be assembled into a buckypaper (Fig. 1b) and have qualitatively high purity based on SEM imaging (Fig. 1c).

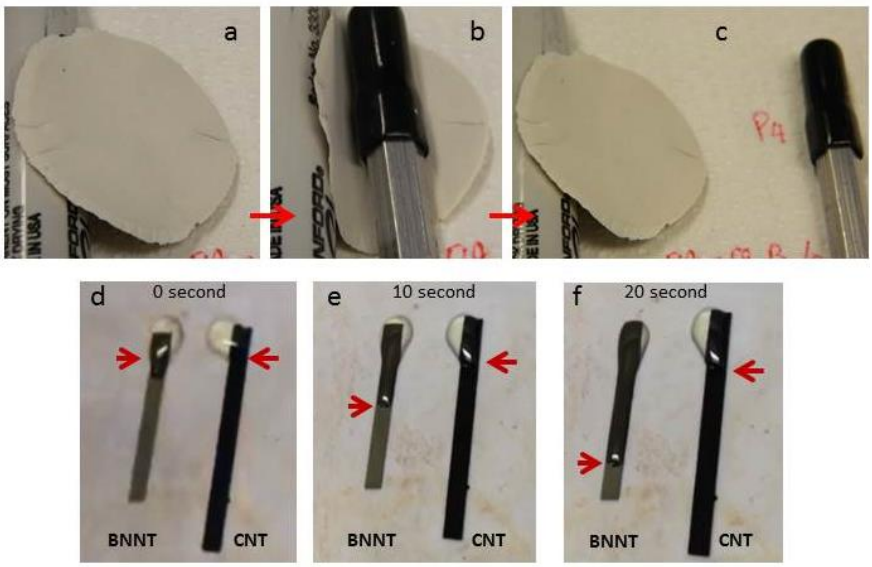

Fig. 2: (a, b and c): Strong and flexible BNNT buckypaper with good recovery and no visible creasing in multiple bending cycles; (d, e and f): wettability comparison of BNNT and CNT buckypapers with epoxy resin [21]

Method of epoxy nanocomposite thin film preparation: As an example of the typical experimental procedure for a 3 wt% loading case: 834 mg of purified BNNTs as shown in Fig. 3b (purity assessed with SEM analysis shown in Fig. 3a) were dispersed in ~ 175 ml of acetone, firstly, by grinding BNNT coarse powder/blocks into a fine powder in a small amount of acetone and then bath-sonicating for 30 minutes at a time with the remaining acetone in a cap-container until a well-dispersed suspension formed; secondly, to the BNNT-dispersion in acetone, a small portion (~5g) of total amount (24 g) of Epon828 was mixed by magnetically stirring to passivate the BNNTs in a diluted epoxy resin environment in order to reach a maximal debundle with the aid of resin in acetone solution. The mixture was continuingly stirred overnight at room temperature and then bath-sonicated for 30 min. Finally, the remaining epoxy resin was added into the mixture, and the mixture was stirred for additional 6 h at room temperature and 3 h at 60 °C. Afterward, the acetone solvent was removed with nitrogen under stirring at 60 °C, and the residue mixture was dried in a vacuum oven at 80 °C for 8 h to further remove any remains of solvent and then cooled to room temperature under nitrogen.

Curing procedure: The solvent-free BNNT-epoxy resin was mixed with curing agent (Epikure 3223), at 12 PPH resin by weight, using a planetary centrifugal mixer (Thinky ARE 310) as shown in Fig. 3d for 1 min at 2000 RPM and degassed at 2200 RPM for 30 seconds. The well-mixed liquid

sample was casted on a borosilicate glass plates treated with a release agent (Frekote 770-NC, part No. 83469). A second glass plate was used to compress the resin and a 200 µm metal shim was placed between the two glass plates to control the film thickness as demonstrated in Fig. 3e and f. Once the top glass plate was carefully and slowly laid down (to minimize trapping air-bubble), a heavy block was placed on top of the glass plate. The sample was kept at room temperature for 48 h, after which it was post-cured in an air-oven to warm up for 1 h from room temperature to 120 °C and additional 2h for post curing at 120 °C. After cooling to room temperature, the thin film sample was removed from the glass plate. CNT-epoxy samples were prepared and cured in the same way as the BNNT-epoxy composites. As demonstrated in Fig. 3g and h, the fully cured BNNT-epoxy thin films have pretty good transparency with the thickness up to 430 µm (Fig. 3g) and BNNT loading up to 4 wt% (Fig. 3h), while CNT-epoxy thin films are completely non-transparent even at low CNT loading and low thickness.

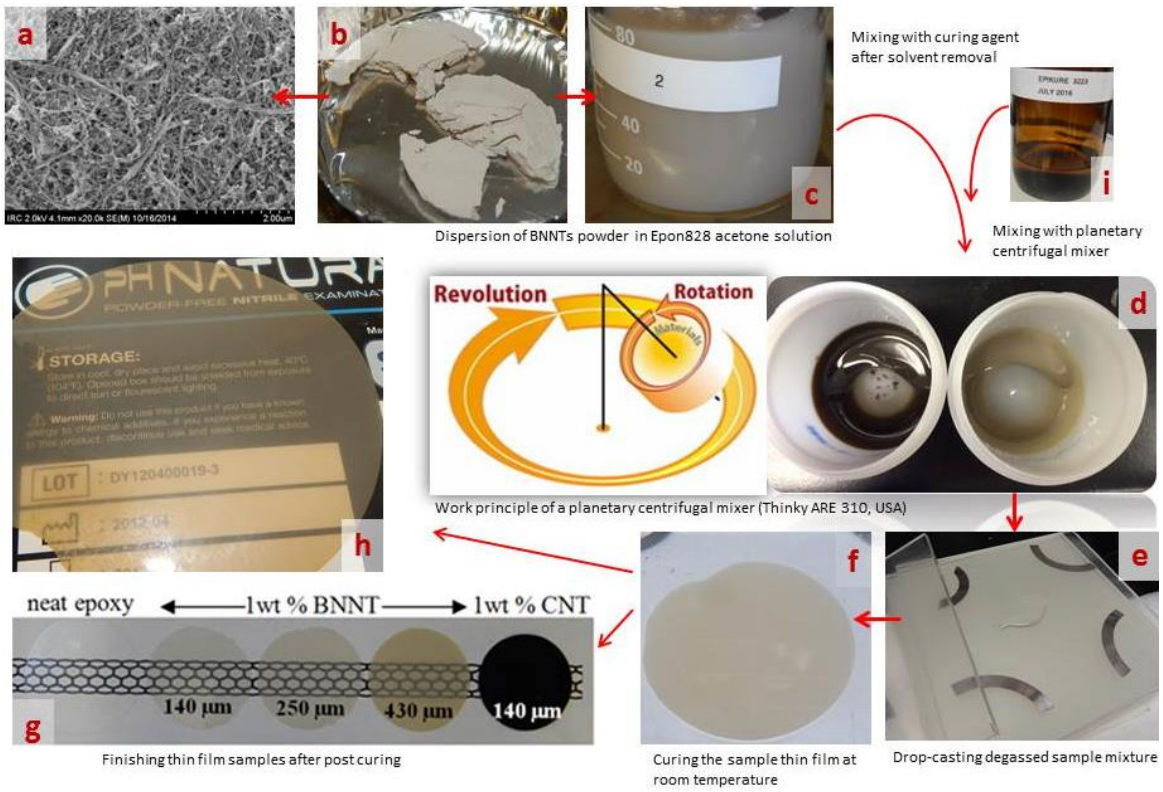

Fig. 3: a) SEM analysis of purified BNNT material; b) purified BNNT starting material, c) suspension of BNNTs in acetone and Epon828, d) planetary centrifugal mixing and work principle, e) drop-casting on borosilicate glass plates, f) cured thin film at room temperature between the two glass plates, g) fully cured thin films (1 wt% of CNTs, BNNTs and neat epoxy with different thickness), h) 4 wt% of BNNTs at thickness of 200 µm, i) curing agent Epikure 3223.

Tensile characterization: A micro-tensile test frame (Fullam Substage Test Frame) was used to measure the mechanical properties of the fabricated thin films. At least five dogbone specimens, according to ISO 527-2 (Type 1BB), were punched out from each thin film sample and tested. For all tests a displacement rate of 1 mm/min was used. Glass transition temperature (T_g) was measured by dynamic mechanical thermal analysis (DMA).

Fracture toughness characterization: Plane-strain fracture toughness (K_{IC}) was measured using five rectangular specimens of 2×4×20 mm. A precision saw was used to create a notch of ~ 1×2 mm on samples and the notch was then sharpened with a fresh razorblade. A micro-tensile test frame (Fullam Substage Test Frame) was used to perform a 3-point fracture toughness test at a displacement rate of 3 mm/min.

3 RESULTS AND DISCUSSION

BNNTs and CNTs are structurally and microscopically similar as demonstrated in Fig. 1, however, the heteroatomic construction of B and N atoms in BNNTs and their different affinities resulted in a polarization of B-N bonds and a large bandgap, which differentiate from homo-carbon-atom built CNTs. Such differences may offer some advantages of BNNTs with a better wettability and interface compatibility with applied matrix, therefore, uniform dispersion can be achieved to minimize tube agglomeration and phase separation in composite samples. As demonstrated in Fig. 2d, e and f, BNNTs have faster uptake of epoxy resin by capillary force than CNTs, implying that BNNT-epoxy composite have a better interface interaction.

It is also of interest in this study to examine the effects of impurities in the raw BNNT materials on the transparency and the mechanical performance by comparing with purified BNNTs with small functional groups such as OH. Due to the elemental boron impurity generated during the production of raw BNNT material and the other BN impurities, buckypapers of raw BNNTs (see Fig. 2d, e and f), the epoxy impregnated buckypapers and the raw-BNNT-epoxy thin films are grey or dark brown in appearance. However, once the elemental boron and other BN impurities are removed, or even partially removed, the BNNT buckypaper became whiter (Fig. 1e) and the epoxy composite films became much more transparent (Fig. 3g), even at the loading as high as 4 wt% of BNNTs (Fig. 3h, ~200 μm in thickness).

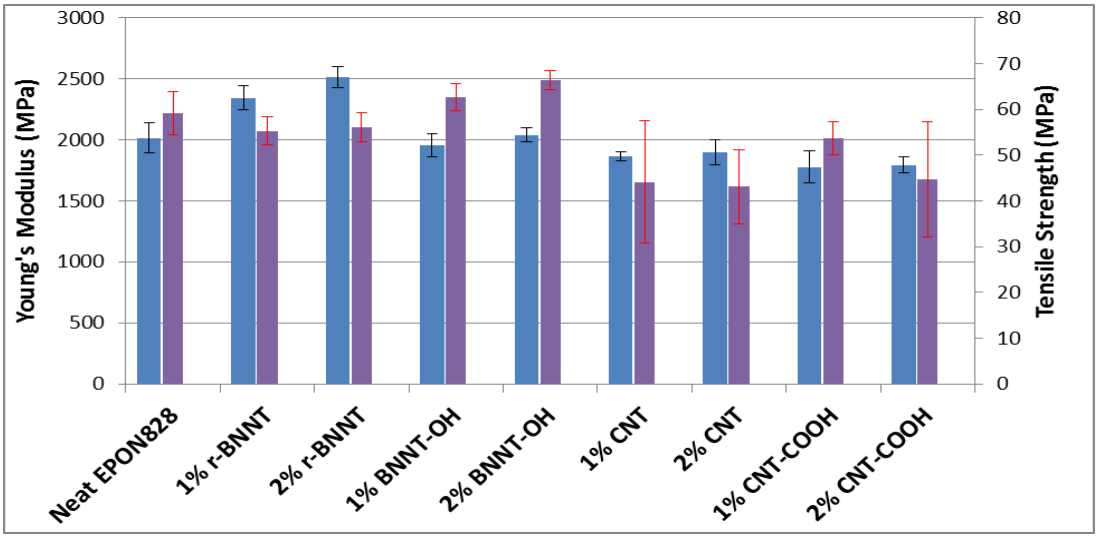

Fig. 4: Young's modulus (blue) and tensile strength (purple) comparison of r-BNNT-Epon828, BNNT-OH-Epon828, CNT-Epon828 and CNT-COOH-Epon828 at 1 and 2 wt%.

The experimental measurements of tensile properties (Fig. 4) show that the Young's modulus of the CNT-Epon828 composites is consistently lower than the neat epoxy and BNNT-epoxy composites. The best Young's modulus for the CNT composites at 1 or 2 wt% loading are about 6% lower than the neat sample, while the raw BNNT composite at 2 wt% has Young's modulus about 25% higher than the neat Epon828. The OH-functionalized BNNT composite has equal to or slightly higher Young's modulus than the neat one. In the case of tensile strength, both CNT composites at 1 wt% and 2 wt% loading have tensile strength about 25~27%, 21 ~23% and 29~35% lower than the neat epoxy, r-BNNT and BNNT-OH samples, respectively. The raw BNNT composites at both 1 and 2 wt% loading have about 5~7% tensile strength lower than the neat epoxy sample. Clearly, the OH-functionalized BNNT composites at 1 and 2 wt% loading have obvious improvement of tensile strength and the best performance at 2 wt% loading is about 12% higher than the neat sample suggesting that some binding effect of OH group to the epoxy matrix might occur.

In addition, as shown in Fig. 4, Young's modulus and tensile strength of CNT-COOH composites are apparently decreased when compared to the neat epoxy sample, suggesting that the acid

functionalized CNTs may be significantly damaged (e.g. by shortening the tubes and generating more defects through concentrated acid treatment), decreasing the effectiveness of CNTs as nanofillers for reinforcement, although acid functionalized CNTs have much better dispersion and solubility than raw CNTs. However, the tensile strength of acid functionalized CNT-epoxy composites are slightly higher than the raw CNT composite, which may indicate that the acid surface functional groups may have certain interaction with the epoxy matrix.

Fig. 5 compares nanocomposites containing r-BNNT up to 7 wt% and BNNT-OH up to 5 wt%. As shown in Fig. 5, the Young's modulus of both r-BNNT and BNNT-OH composites are higher than the neat epoxy resin. With the increase of BNNT loading, both the raw and functionalized BNNT composites have consistent increases of Young's modulus. The raw BNNT composites at 5 and 7 wt% loading have the most improvement of Young's modulus with an increase about 35%. The best improvement for BNNT-OH composite is about 21% at 5 wt% loading. It is notable that the raw BNNT composites have considerably higher Young's modulus to the OH-functionalized BNNT composites overall of all samples, and the difference for the best sample is about 14%. However, both groups of samples have a consistent trend of increased Young's modulus with the increase of nanotube loading. It was expected that the purified and functionalized BNNTs would have better interaction with epoxy matrix; therefore, those composites should have a better performance. One factor is to be considered that raw BNNTs could have a high population of individual BNNTs or small bundles due to impurities deposited on tube surfaces, which could provide an advantage for a better dispersion in the matrix, while the purified BNNTs form big bundles (see Fig. 1f) and may have agglomeration. Conversely, all the raw BNNT composites from 1 to 7 wt% loading have consistent decrease of the tensile strength that are lower than the neat epoxy resin and the BNNT-OH composites from 1 to 5 wt% loading. The BNNT-OH composites have impressive improvement through all the samples, and the best performance is about 12% improvement at 2 wt% loading compared with the neat epoxy sample. Both groups of samples do not have the same trend of tensile strength with the nanotube loading changes, although bath groups have decreased tensile strength after 2 wt% with a further increase of nanotube loading.

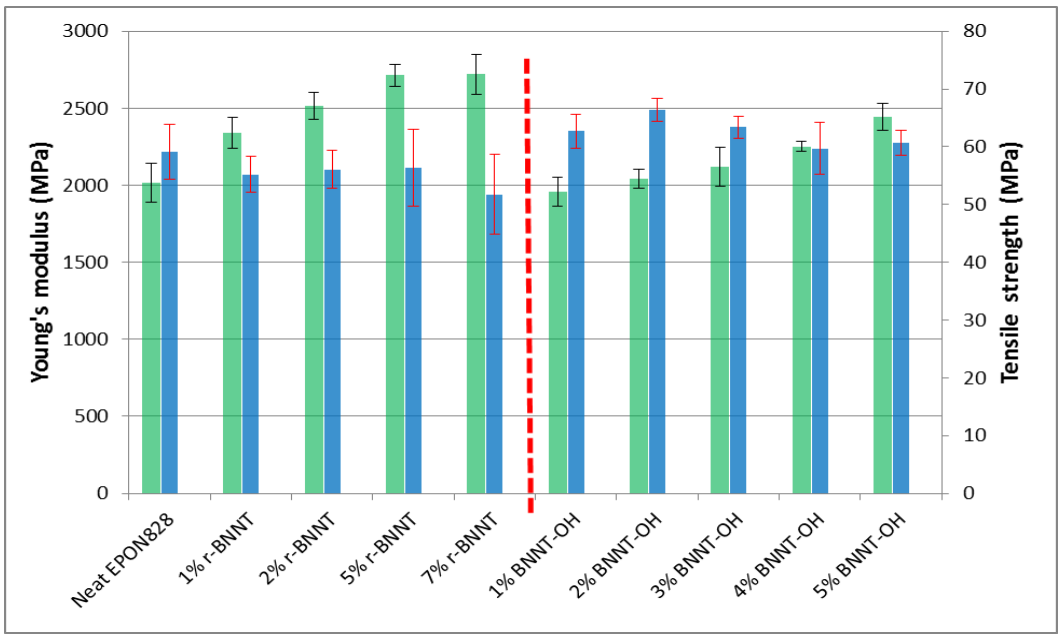

Fig. 5: Comparison of Young's modulus (green) and tensile strength (blue) for neat Epon828, raw BNNT (r-BNNT) and OH-functionalized BNNT (BNNT-OH) Epon828 composites.

Figure 6 demonstrated the tensile toughness and modulus of resiliency for both groups of r-BNNT and BNNT-OH composites. The tensile toughness of r-BNNT composites is systematically decreased with the loading increase compared to the neat epoxy resin. The largest decrease is about 70% and each sample from 1 wt% to 7 wt% is about 10 to 20 % diminish of the tensile toughness. In opposite

way, the modulus of resiliency of each r-BNNT composite is largely improved compared to the neat resin. The best improvement is about 112%, and each sample from 1 to 5 wt%, the step of increase is considerably impressive. The 5 wt% addition of r-BNNT increased both Young's modulus and tensile stress at yield, which eventually lead to significantly increase in modulus of resiliency. The BNNT-OH composites are in generally improving the tensile toughness. The best improvement is about 49% at 2 wt% loading. The largest negative improvement is about -12% at 4 wt% loading. It is clearly different from the r-BNNT composites that the modulus of resiliency of BNNT-OH composites has the same change trend to the tensile toughness with the increase of nanotube loading. The best improvement is about 40% at 2 wt% loading. In contrast to the r-BNNT composite sample, the modulus of resiliency of the 5 wt% BNNT-OH sample decreases only 0.5 % compared with the neat epoxy sample.

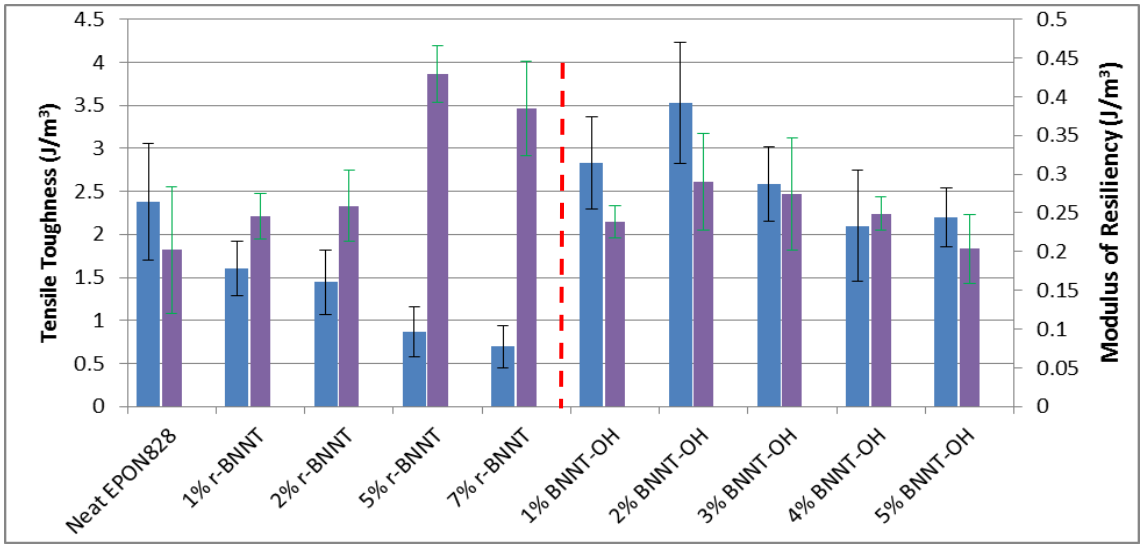

Fig. 6: Comparison of tensile toughness (blue) and modulus of resilience (purple) between neat Epon828, raw BNNT epoxy composites and OH-functionalized BNNT composites.

Figure 7 demonstrates that the glass transition temperature (T_g) considerably and consistently increased with the increase of the r-BNNT loading. The highest increase is the sample at 7 wt% r-BNNT about 43 ^{o}C above the neat epoxy sample. In contrast, all the OH-functionalized BNNT composites remained almost unchanged in T_g relative to the neat epoxy resin (~ 151 ^{o}C). It is unclear what caused such dramatic increase in the glass transition temperature of r-BNNT composite, but the difference between raw and purified BNNTs indicates the impurities likely play a role. It is uncertain to say yet that BNNTs do not affect the glass transition temperature in a composite. As shown in Fig. 7, the effect of the functionalized BNNTs on their epoxy composites is significantly different from the raw BNNT composite in strain at break. The composite at 2 wt% BNNT-OH loading had the highest strain at break improvement about 22% higher than the neat Epon828. With the further loading increase of functionalized BNNTs after 2 wt%, the strain at break slowly decreased and the lowest value is about 15% lower for the 4 wt% loaded BNNT-OH composite than the neat epoxy sample. Conversely, the r-BNNT composites (1 to 7 wt%) have almost an exponential drop in the strain at break. The closest drop to the neat epoxy is about 29 % at 1 wt% loading and the lowest drop is about 62% at 7 wt% loading. It is quite clear that the specimens with BNNT-OH reinforced composite have improved strain at break for a certain nanotube loading range and hence tensile toughness comparable to neat epoxy (even at the highest BNNT-OH loading of 5 wt%)

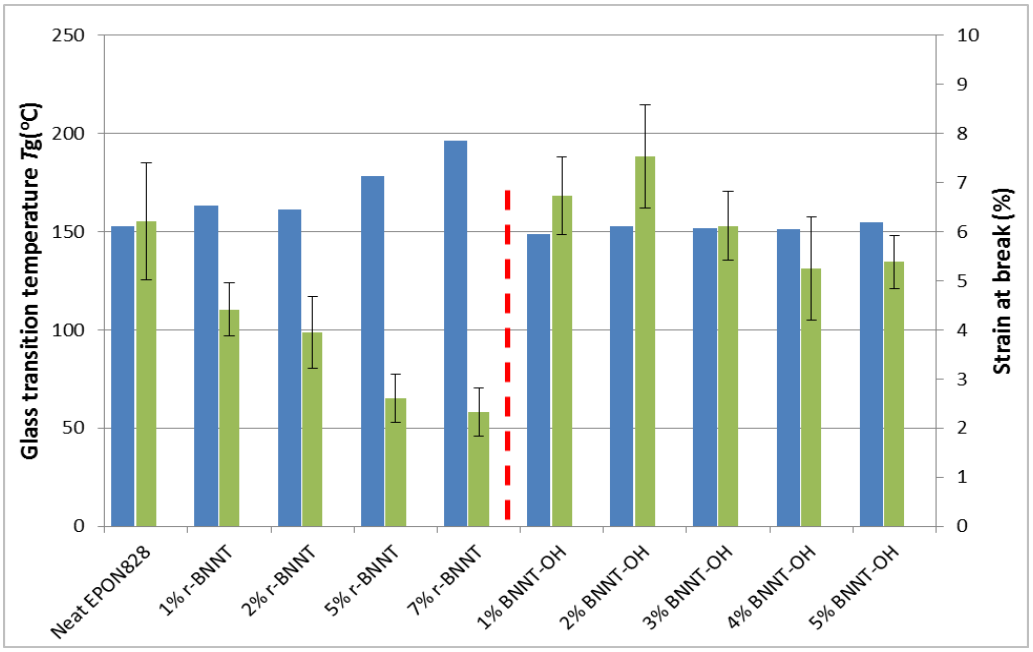

Fig. 7: Comparison of Glass transition temperature (blue) and strain at break (green) between neat Epon828, r-BNNT- and BNNT-OH composites

From the fracture toughness results shown in Fig. 8, the r-BNNT composites have linearly increased fracture toughness with the loading increase up to 5 wt%, and the best improvement of the fracture toughness at 5 wt% loading is about 43%. Although at the loading of 7 wt% of r-BNNT the fracture toughness has a slight drop compared to the 5 wt% sample, it still has about 38 % improvement to the neat epoxy sample. The BNNT-OH composites also have comparable fracture toughness improvement to the neat sample and to the r-BNNT composite samples at the similar loading of BNNTs. In the CNT case, the raw CNT composites have similar and comparable fracture toughness, only the acid functionalized CNT have slightly decreased fracture toughness to the neat epoxy sample.

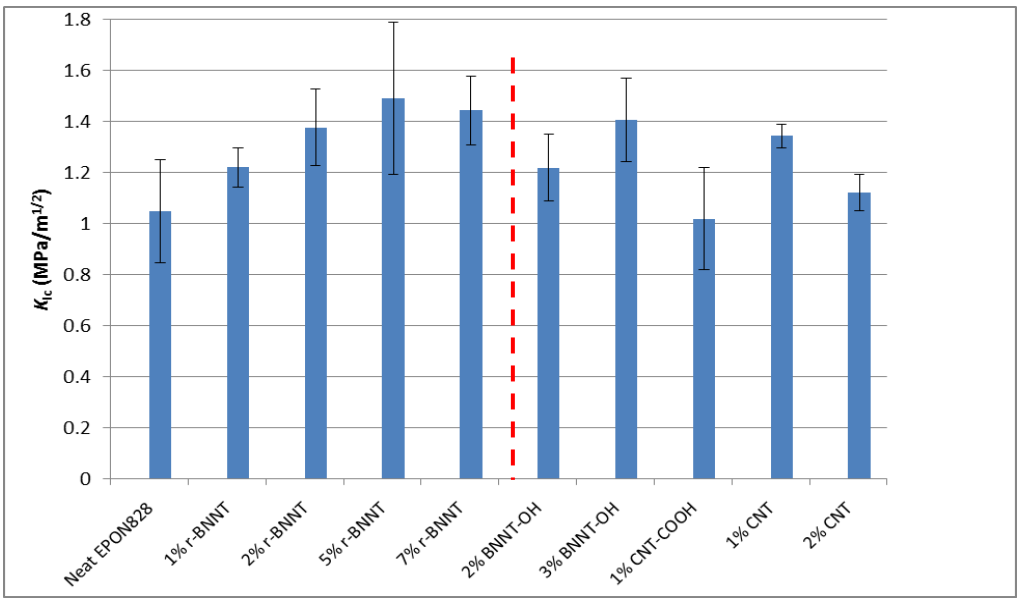

Fig. 8: Comparison of Fracture toughness between neat, BNNT- and CNT-composites

4 CONCLUSIONS

This parallel study of BNNT- and CNT-Epon828 composites revealed that BNNTs show better wettability with epoxy resin than CNTs, therefore, BNNT composites have a better loading transfer due to a better interface compatibility. It is hard to obtain a transparent thin film of appreciable thickness (within a few hundred micron meter thickness) with 1 wt% CNT loading, while 1 wt% (even up to 4 wt%) purified and functionalized BNNT composite thin film can provide excellent transparency for thickness of several hundred microns. The OH-functionalized BNNT composites may have not yet reached to the best dispersion due to large bundles with high purity compared with raw BNNTs, however, the overall mechanical performance, including higher strength and maximum strain compared to r-BNNT composites, seems to indicate that the purified and functionalized BNNTs are promising for future study. More covalent surface functionalization (e. g, a variety of functionalization types and degrees of functionalization) needs to be carried out to optimize for a better load transfer and hence achieve the best mechanical performance for the composite.

ACKNOWLEDGEMENTS

The authors thank Mr. Gordon Chan (NRC) for the SEM imaging. Funding to support synthesis of BNNTs and development of BNNT composites was provided by the National Research Council Canada through the Security Materials Technology Program.

.

REFERENCES

[1] J.N. Coleman, U. Khan, W.J. Blau and Y.K. Gun'ko, Small but strong: A review of the mechanical properties of carbon nanotube-polymer composites, *Carbon,* **44**, 2006, pp. 1624-1652.

[2] D. Golberg, Y. Bando, Y. Huang, T. Terao, M. Mitome, C. Tang and C. Zhi, Boron nitride nanotubes and nanosheets, *ACS Nano*, **4**(6), 2010, pp. 2979-2999.

[3] B. Ashrafi, J.W. Guan, V. Mirijalili, Y. Zhang, C. Li, P. Hubert, B. Simard, C.T. Kingston, O. Bourne and A. Johnston, Enhancement of mechanical performance of epoxy/carbon fibres laminate composites using single-walled carbon nanotubes, *Composites Science and Technology*, **71**(13), 2011, pp.1569-1598.

[4] M. Rahmat and P. Hubert, Carbon nanotube-polymer interactions in nanocomposites: a review, *Composites Science and Technology*, **72**(1), 2011, pp. 72-84.

[5] J.W. Guan, B. Ashrafi, Y. Martinez-Rubi, Y. Zhang, C.T. Kingston, A. Johnston and B. Simard, Integration of single-walled carbon nanotubes into a single component epoxy resin and an industrial epoxy resin system, *Polymer & Polymer Composites*, **19**(2&3), 2011, pp. 99-106.

[6] B. Ashrafi, J.W. Guan, V. Mirijalili, P. Hubert, B. Simard and A. Johnston, Correlation between Young's modulus and impregnation quality of epoxy-impregnated SWCNT buckypaper, *Composite Part A: Applied Science and Manufacturing*, **41**(9), 2010, pp. 1184-1191.

[7] Y. Martinez-Rubi, B. Ashrafi, J.W. Guan, C.T. Kingston, A. Johnston, B. Simard, V. Mirjalili, P. Hubert, L. Deng and R. Young, Toughening of epoxy matrices with reduced single-walled carbon nanotubes, *ACS Appl. Mater. Interfaces*, **3**, 2011, pp. 2309-2317.

[8] E. Najafi, J. Wang, A. P. Hitchcock, J.W. Guan, S. Denommee and B. Simard, Characterization of single-walled carbon nanotubes by scanning transmission X-ray spectromicroscopy: purification, order and dodecyl functionalization, *J. Am. Chem. Soc.*, **132**, 2010, pp. 9020-9029.

[9] A.T. Nasrabadi and M. Foroutan, Interaction between polymers and single-walled boron nitride nanotubes: a molecular dynamics simulation approach, *J. Phys. Chem. B.*, **114**, 2010, pp. 15429-15436.

[10] S. Rouhi, Molecular dynamics simulation of the adsorption of polymer chains on CNTs, BNNTs and GaNNTs, *Fibers and Polymers* **17**, 2016, pp. 333-342.

[11] K.S. Kim, M.B. Jakubinek, Y. Martinez-Rubi, B. Ashrafi, J.W. Guan, K. O'Neill, M. Plunkett, A. Hrdina, S. Lin, S. Denommee, C.T. Kingston and B. Simard, Polymer nanocomposites from free-standing, macroscopic boron nitride nanotube assemblies, *RSC Advances*, **5**, 2015, pp. 41186-41192.

[12] X. Chen, L. Zhang, C. Park, C.C. Fay, X. Wang, and C. Ke, Mechanical strength of boron nitride nanotube-polymer interfaces, *Appl. Phys. Lett*. **107**, 2015, pp. 253105.

[13] W. Meng, Y. Huang, Y. Fu, Z. Wang and C. Zhi, Polymer composites of boron nitride nanotubes and nanosheets, *J. Mater. Chem.***C2**, 2014, pp. 10049-10061.

[14] M.F.L. De Volder, S.H. Tawfick, R.H. Baughman and A.J. Hart, Carbon nanotubes present and future commercial applications, *Science*, **339**, 2013, pp. 535-539.

[15] K.S. Kim, C.T. Kingston, A. Hrdina, M.B. Jakubinek, J.W. Guan, M. Plunkett and B. Simard, Hydrogen-catalyzed, pilot-scale production of small-diameter boron nitride nanotubes and their macroscopic assemblies, *ACS Nano*, **8**(6), 2014, pp. 6211-6220.

[16] M.W. Smith, K.C. Jordan, C. Park, J.W. Kim, P.T. Lillehei, R. Crooks and J.S. Harrison, Very long single- and few-walled boron nitride nanotubes via the pressurized vapor/condenser method, *Nanotechnology*, **20**, 2009, pp. 505604 (6pp).

[17] A. Fathalizadeh, T. Pham, W. Mickelson and A. Zettl, Scaled synthesis of boron nitride nanotubes, nanoribbons, and nanocomcoons using direct feedstock injection into an extended pressure, inductively-coupled thermal plasma, *Nano Letters*, **14**, 2014, pp. 4881-4886.

[18] M.B. Jakubinek, J.F. Niven, M.B. Johnson, B. Ashrafi, K.S. Kim, B. Simard and M.A. White, Thermal conductivity of bulk boron nitride nanotube sheets and their epoxy-impregnated composites, *Phys. Status Solidi A*, **213**(8), 2016, pp. 2237-2242.

[19] K.S. Kim, M.J. Kim, c. Park, C.C. Fay, S.H. Chu, C.T. Kingston and B. Simard, Scalable manufacturing of boron nitride nanotubes and their assemblies: a review, *Semicond. Sci. Technol.*, **32**, 2017, pp. 013003 (18pp).

[20] Y. Martinez-Rubi, Z.J. Jakubek, M.B. Jakubinek, K.S. Kim, F. Cheng, M. Couillard, C.T. Kingston and B. Simard, Self-assembly and visualization of poly(3-hexyl-thiophene) chain alignment along boron nitride nanotubes, *J. Phys. Chem. C*, **119**, 2015, pp. 26605-26610.

[21] B. Ashrafi, et al., Processing and properties of epoxy-impregnated boron nitride nanotube buckypaper, in submitting.

[22] J.W. Guan and B. Simard, Raw BNNTs purification protocols in brief (unpublished process): raw BNNTs were dispersed in liquid phase to remove most of h-BN left over feedstock, new formed amorphous BN flakes/particles, organic/polymeric BN species by extraction and separations, and finally remove elemental boron particles. Purified BNNTs can be treated with halogen treatment to have a surface functionalization by breaking B-N bonds on the outer surface layer. For details please contact the authors.